A Low-Thrust-Enabled SmallSat Heliophysics Mission to Sun-Earth L5

Natasha Bosanac
University of Colorado Boulder
431 UCB
Boulder, CO, 80309
303-492-7061
natasha.bosanac@colorado.edu

Farah Alibay
Jet Propulsion Laboratory
California Institute of Technology
4800 Oak Grove Dr.
Pasadena, CA 91109
818-354-2778
farah.alibay@jpl.nasa.gov

Jeffrey R. Stuart
Jet Propulsion Laboratory
California Institute of Technology
4800 Oak Grove Dr.
Pasadena, CA 91109
818-354-2778
Jeffrey.r.stuart@jpl.nasa.gov

Abstract— **We present an approach to enable SmallSat mission concepts to the Sun-Earth (SE) L_5 Lagrange point in support of advancing our understanding of solar processes and weather monitoring capabilities by addressing one of the primary challenges of such a mission: traveling to this distant region with limited propulsive capability. Heliophysicists have long been interested in missions to SE L_5, which trails behind the Earth in its orbit, due to the capability for viewing solar and interplanetary phenomena. Consequently, a spacecraft orbiting in the vicinity of SE L_5 would observe the Sun before it rotates into Earth nadir and provide early warning of solar activity.**

Although SmallSats have emerged as an effective and low-cost platform for space-based science and exploration, operational and mission constraints create significant challenges during the trajectory design process. For instance, the miniaturization of electrospray and ion thrusters render low-thrust propulsion systems an enabling technology for upcoming small satellite missions. However, such systems supply only a low acceleration over limited time intervals. Furthermore, the deployment conditions associated with a SmallSat are typically determined by the primary mission and may evolve frequently throughout the lifecycle of the mission. These regular updates may result in deviations from an individual reference trajectory that are too large for a low-thrust propulsion system to overcome, thereby necessitating a complete trajectory redesign. Together, these operational and mission constraints severely impact the geometry and availability of feasible trajectories that deliver a low-thrust-enabled SmallSat from an uncertain deployment state to the vicinity of SE L_5. In fact, these challenges necessitate a rapid and well-informed procedure that leverages dynamical systems techniques for trajectory design. We summarize and demonstrate such an approach within this paper.

TABLE OF CONTENTS

1. INTRODUCTION

Understanding the mechanisms behind the acceleration of Solar Energetic Particles (SEPs) in Coronal Mass Ejections (CMEs) is a key priority for the heliophysics community [1]. In particular, observing these CMEs outside the Earth-Sun line would help us better understand the structure of the shock fronts. Additionally, CMEs are the main driver for space weather; solar storms can cause havoc to the satellite systems we have come to rely on and being able to better forecast such storms will soon become invaluable.

The Sun-Earth (SE) L_5 Lagrange point (or SEL_5) offers a unique vantage point for observing CMEs since it is 60 degrees off the S-E line and trails behind Earth in its orbit. A spacecraft placed at this point would therefore not only provide a new observation point for science measurements, but it would also be able offer an early warning system for solar weather. Thus far, the only mission that has observed the Sun from such a position has been the STEREO spacecraft [2], which drifted through the points in their orbit. No mission has ever been permanently positioned at these points. This is in part driven by the technology challenges involved with reaching such a destination, which in turn drives the cost of such a mission.

In this paper, we address the challenges involved with the journey from the Earth to the SEL_5 point. We offer a solution that would enable a SmallSat platform to reach such a destination using current spacecraft technology and limited propulsive capability. To this end, we first start by describing the science motivation behind a mission to SEL_5. We then present the current state-of-the-art in SmallSat (and CubeSat – in this paper we refer to CubeSats as a subset of the SmallSat family) propulsion and power systems, thereby producing a design constraint matrix. We then present the principles behind Dynamical Systems Theory (DST) and demonstrate how these techniques enable spacecraft with lower propulsive capability to reach previously inaccessible destinations. DST, combined with the design constraint matrix, is used to present an initial trajectory to SEL_5, which is representative of the type of trajectories that could be developed using an informed trajectory design approach.

978-1-5386-2014-4/18/$31.00 ©2018 IEEE

2. Science Motivation

CMEs are expulsions of plasma and magnetic flux from the solar corona, which cause SEPs to be accelerated throughout the solar system at speeds ranging from 200 to 3000 km/s. Their occurrence varies with the solar cycle, which is an 11-year solar magnetic activity cycle. During solar maximum, multiple CMEs can occur every day [3]. Despite this frequent occurrence, the heliophysics community still has a limited understanding of the sources of particle acceleration in CMEs. The heliophysics decadal survey [1] identified two key goals related to CMEs [4]:

1. To understand particle acceleration in coronal mass ejections (process and characteristics). In particular, there is a desire to understand where CME-driven shocks form and how they affect particle acceleration, as well as establishing more specifically what drives particle acceleration and propagation through the solar system.
2. To observe the evolution of the magnetic field when CMEs erupt and to constrain existing models of the magnetic reconnection that occurs.

In addition to these key science goals, CMEs are also the main driver for solar weather. CMEs produce geomagnetic storms, which in turn induce currents in the ionosphere. A large storm could result in significant damage to satellites, radio communications, and even power grids. Moreover, SEPs generated in CMEs are highly energetic and can endanger life, particularly those of potential interplanetary astronauts who would not be shielded by the Earth's magnetic field, as well as causing single-event upsets which can destroy spacecraft electronics. Therefore, gaining a better understanding of the characteristics of CMEs could help us better predict solar weather and protect assets, especially if an advance warning system were available to predict weather before it hit the Earth.

The key parameters when trying to understand particle acceleration are the time and velocity of arrival of particles [5]. Most current observation platforms are either in Earth orbit, or at the nearby SEL_1 or SEL_2 points. The limitation of these observations is that they are single points directly in the Earth-Sun line, and therefore only provide limited visibility into the 3D structure of the CMEs. This structure can be better observed by placing an observation platform in an Earth-leading or Earth-trailing orbit, as shown in Figure 2. Of particular interest in this region are the SEL_4 and SEL_5 points. At these locations, minimal propulsive capability is therefore required to maintain bounded motion near these points.

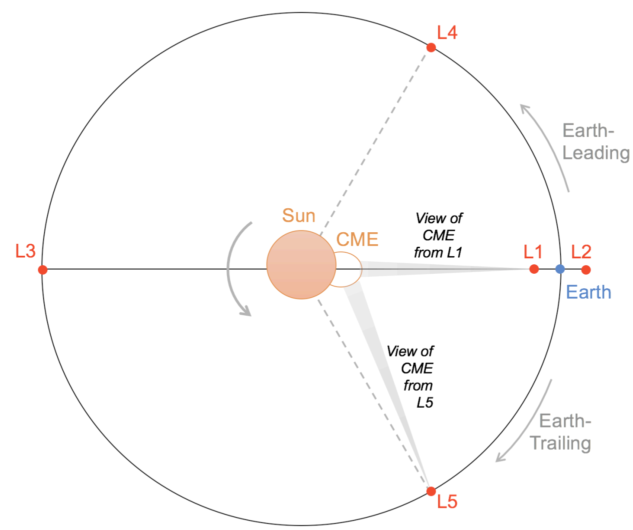

Figure 2. Lagrange Point Geometry – SEL_4 and SEL_5 offer unique vantage points for observing CMEs.

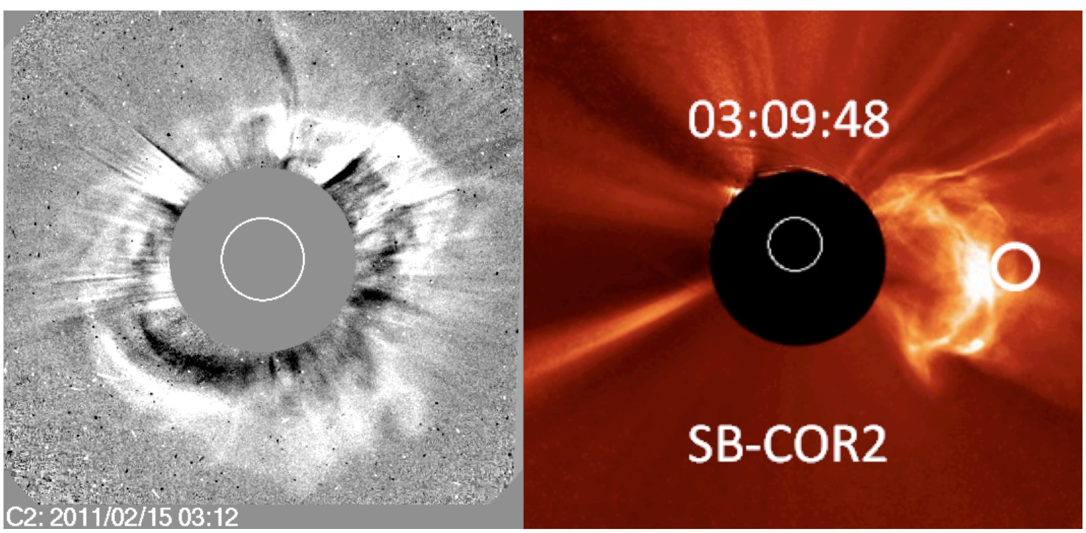

Figure 1. Images from SOHO (left, at SEL_1) and STEREO-B (right, trailing ~90º behind Earth) taken at the same time. While the CME cannot be observed by SOHO, it can very clearly be seen in the STEREO image [6]

The only mission thus far to have observed the Sun from such positions is the Solar Terrestrial Relations Observatory (STEREO) mission [2]. This pair of spacecraft only drifted through the SEL_4 and SEL_5 points, and did not station-keep at these positions, which would have offered continuous observation of Earth-impacting CMEs. Nevertheless, comparing images from STEREO while outside the SE line with those taken by the Solar and Heliophysics Observatory (SOHO), which is placed at the SEL_1 point, provides clear insight into the observational advantage of placing a spacecraft outside the SE line, as shown in Figure 1.

In addition to being located 60º off the Sun-Earth line, SEL_5 has the advantage over SEL_4 of being in an Earth trailing orbit and lies over the east limb of the Sun as seen from Earth (depicted in Figure 2). The Sun's rotation rate is approximately 13º/day, which means that an observation platform placed at SEL_5 would provide 4-5 days of advance warning of an incoming solar storm. While SEL_4 is directly within the path of SEPs due to the Parker spiral, it lies over the west limb of the Sun and consequently is not as useful for solar weather forecasting. We choose to focus on trajectories to SEL_5 in this paper due to its clear advantage for space weather monitoring, although these methods could easily be extendable to provide trajectories to SEL_4 as well.

3. TECHNOLOGY DRIVERS

As described in the last section, the value of a heliophysics mission to L_5 is widely recognized in the heliophysics community, and several large and smaller mission concepts have been proposed [7,8,9]. However, the cost of such missions has been prohibitively expensive thus far due to several factors that increase the complexity of missions to such a target, as compared to Earth-orbiting missions. First, the spacecraft must leave Earth orbit and navigate to the Lagrange point. This not only leads to challenges in operations, but also puts constraints on the Delta-V and propellant requirements for the mission. Furthermore, once at its destination, the distance from Earth results in challenges associated with speed-of-light delay and space losses for communication. These constraints therefore make it very difficult for a low-cost SmallSat concept to be proposed to achieve this science.

While many CubeSats and SmallSats have been slated to launch to destinations beyond Earth orbit by 2020, including MarCO going to Mars, and Lunar Flashlight, LunaH-Map and Lunar IceCube destined to explore the Moon, one of the main limiting factors for all these designs was their propulsion systems. The design teams for these spacecraft have had to work around severe propulsive capability limitations to achieve the goals of these missions. As they stand, these types of spacecraft would be unable to reach a target such as the SEL_5 (for example, MarCO has a cold gas system with 40 m/s Delta-V, which would be insufficient to reach L_5 from an arbitrary, uncertain deployment condition).

The goal of this paper is therefore to undertake the "getting there" portion of the challenge. Specifically, we investigate how new methods in mission design and navigation for low-thrust systems could become technology enablers in allowing SmallSats to reach such a distant target, thereby reducing the cost of the platform needed to provide such investigations.

To frame this problem, we first present the state-of-the-art in current SmallSat-sized technology for low-thrust propulsion systems and power systems (since the two come hand-in-hand) and produce a design constraint matrix. We aim to uncover a solution space that could be applied to a mission within the next half a decade and therefore constrain ourselves to using existing and upcoming (Technology Readiness Level >4) propulsion technology

Propulsion Systems

SmallSats are defined by their limited mass and volume, often driven by the fact that they are launched as secondary payloads to reduce launch costs. This is particularly limiting for their propulsion systems, which must fit within these allocations. Therefore, to constrain our mission design problem, we investigated the latest available propulsion technologies for SmallSats. Table 1 presents an overview of the different types of propulsion systems, as well as a representative example of an off-the-shelf product that uses this propulsion technology. For each, we also present a typical power requirement and thrust level, which are inputs to the mission design analysis, as well as mass requirements and the type of spacecraft it was intended for.

Power Systems

While solar arrays are now very mature and standard technology for all spacecraft, CubeSats are often limited by volume and surface area when it comes to power. By surveying recent interplanetary CubeSat designs within the

Table 1. Overview of Low-Thrust Propulsion Options for SmallSats and CubeSats

Propulsion Type	Example Providers	Thrust Levels	Power	Mass	Target S/C Size	Ref.
Electrospray	Accion Systems	0.05-1.5 mN	1.5-30W	50g- 1100g	3U-12U CubeSat	[10]
Hall Thruster	BHT 200	13 mN at 200W	100-300W	1.2kg dry + ~2-4kg PPU	SmallSat/ 12U+ CubeSat	[11]
Pulse Plasma Thruster	Aerojet	1.24mN	100 W	4.75kg dry	SmallSat	[12]
Resistojet	Aerojet	36 mN	~625 W	2.87kg dry	SmallSat	[12]
Ion Thruster	JPL MiXI	0.01-1.5 mN	13-50W	0.2kg + ~1-2 kg PPU	SmallSat/ 12U+ CubeSat	[13]

Jet Propulsion Laboratory, we estimate that the typical power availability for 6-12U CubeSats is approximately 35-50W at Earth. In fact, MMA designs [14] offers two types of solar arrays for 6U CubeSats, the Hawk and the eHawk arrays, that provide 36W and 72W at Earth respectively.

For SmallSats, whereas companies such as Orbital ATK offer foldable arrays such as the Ultraflex array [15], energy management is often the limitation. Power processing units (PPUs) can often be large and cumbersome. In addition, having to shunt high loads when not using the propulsion system results in the need for radiators and louvers, which again significantly affect mass. Consequently, to stay within the range of current small PPU developments [16], it is estimated that the maximum power available for a SmallSat architecture should be in the 100-300W range.

Design Constraint Matrix

Of the systems presented in Table 1, the Hall Thruster offers the best thrust level for each watt of power. Furthermore, Glenn Research Center is currently developing an iodine alternative to the xenon-powered BHT-200 which would offer increased performance over the current technology [16]. On the other side end of the size scale, electrospray thrusters are the only low-thrust thrusters that were specifically designed for CubeSats and can fit in the smaller form factors.

Table 2. Design Constraint Matrix

	Form Factor	Max Wet Mass	Avail. Prop Power	Thrust Level	Isp (sec)
Lower End	6U CubeSat	14kg	10W	0.4mN	1250
Upper End	ESPA SmallSat	180kg	200W	13mN	1375

These two systems were therefore picked as our baseline for further investigation, as shown in Table 2. They have the advantage of being at extreme ends of the design envelope in terms of thrust levels, power required, mass, and volume, therefore enabling our method to be broadly applied across the design space.

For the purposes of this study, we aim to limit the propellant mass required to get to an L_5 short period orbit, based on the maximum launch mass. Although both platforms have their advantages, we chose to focus on the “Lower End” option for this paper, as a starting point for the application of DST to this design problem, since it is the most constraining problem in terms of mass. Based on typical 6U CubeSat masses, 4 kg of a maximum wet mass of 14kg was allocated to propellant to further constrain the design problem at hand. Future work will expand this problem to the broader design space to create a method that is widely applicable to this design problem.

4. MISSION DESIGN APPROACH

Efficient and well-informed trajectory design procedures can serve as an enabling technology for complex CubeSat missions beyond low-Earth orbit, potentially mitigating the impact of hardware and operational limitations in the near term [17]. For a low-thrust-enabled mission, miniaturization of the propulsion system to accommodate a CubeSat form factor places significant limitations on the available acceleration and propellant mass. As a result, navigating from an uncertain deployment state to a desired mission orbit creates challenges for trajectory designers. However, an informed approach that actively leverages the natural dynamics within a multi-body system, such as the Sun-Earth-Moon environment, supports rapid itinerary planning and robust trajectory construction during both mission development and after deployment [18].

In a multi-body dynamics approach to trajectory design for the CubeSat mission of interest, we first leverage an approximation of the Sun-Earth system to construct a discontinuous initial guess. The chaotic dynamics with the Sun-Earth environment are well-approximated via a Circular Restricted Three-Body Problem (CR3BP). In this autonomous dynamical model, fundamental structures such as periodic and quasi-periodic orbits and their associated manifolds guide natural flow within the system. We can rapidly compute and evaluate these structures in the CR3BP via DST. Their impact on trajectories within the Sun-Earth system can offer us guidance into the general itinerary for a low-thrust-enabled CubeSat as it travels from a fixed deployment state to the desired mission orbit. Furthermore, we can select such structures and assemble them to construct an initial guess for a trajectory. Incorporating low-thrust arcs, along with a corrections algorithm, enables recovery of a continuous end-to-end trajectory that retains the desired geometry. Such persistence of the trajectory geometry is possible because the underlying dynamical structures, computed in a Sun-Earth CR3BP, often approximately exist when the true ephemerides of the Sun and Earth are considered, and additional gravitational and non-gravitational forces are added [19].

In this section, we summarize the fundamental components of a DST approach to trajectory design for a low-thrust-enabled CubeSat. We present a brief overview of the dynamical models employed during trajectory construction, as well as the procedure used to correct a trajectory consisting of both natural and low-thrust-enabled arcs. We then discuss fundamental dynamical structures relevant for itinerary planning. Structures of interest are also analyzed and assembled to produce a discontinuous initial guess. We correct this guess in a point mass ephemeris model of the Sun and Earth, with natural and low-thrust-enabled arcs.

We construct a sample trajectory using this process for a 14kg CubeSat and a 0.4mN low thrust engine (“Lower End” option in the Design Constraint Matrix). Throughout this paper, we assume a deployment condition similar to a previous state for the Exploration-Mission 1 (EM-1) CubeSats, corresponding to an epoch of 9 Oct 2018 [17]. This deployment condition corresponds to a high-energy trajectory that begins near the Earth and performs a close flyby of the Moon. Fixing the deployment condition to a sample state and epoch will significantly constrain the trajectory design space. While the constructed trajectory represents only a single solution in a vast and diverse solution space, it serves as a demonstration of the value in applying a DST approach to trajectory design for low-thrust-enabled CubeSat missions.

Dynamical Models

The most fundamental model used in a multi-body dynamics approach is the autonomous CR3BP, which captures the point mass gravitational influences of the Sun and Earth, acting on a spacecraft with negligible mass. The Sun and Earth are assumed to travel along circular orbits about their mutual barycenter. Then, to recover an autonomous system, we employ a frame $\hat{x}\hat{y}\hat{z}$ that rotates with the Sun and the Earth. In addition, we nondimensionalize length, mass and time quantities such that the distance between the Earth and Sun is equal to unity, the mass of the Earth is equal to μ, and the mean motion of the primaries in their circular orbits is also unity. With these fundamental assumptions, we can write the equations of motion for a spacecraft, located at the nondimensional coordinates (x,y,z) relative to the barycenter, in a rotating frame as:

$$\ddot{x} - 2\dot{y} = \frac{\partial U}{\partial x}$$

$$\ddot{y} + 2\dot{x} = \frac{\partial U}{\partial y} \quad (1)$$

$$\ddot{z} = \frac{\partial U}{\partial z}$$

where:

$$U = \frac{1}{2}(x^2 + y^2) + \frac{1-\mu}{r_1} + \frac{\mu}{r_2} \quad (2)$$

is the pseudo-potential function, while:

$$r_1 = \sqrt{(x+\mu)^2 + y^2 + z^2} \quad (3)$$

and

$$r_2 = \sqrt{(x\text{-}1+\mu)^2 + y^2 + z^2} \quad (4)$$

are the distances between the spacecraft and the Sun and the Earth, respectively [20].

Given the assumptions used to construct the equations of motion, the CR3BP is autonomous. As a result, this dynamical model admits an energy-like quantity commonly labeled the Jacobi constant, $C_J = 2U\text{-}\dot{x}^2\text{-}\dot{y}^2\text{-}\dot{z}^2$. At a selected value of the Jacobi constant, natural solutions are restricted to limited regions of the phase space. An infinite set of points that possess a velocity of zero and a nonzero acceleration form zero velocity surfaces in three dimensions. At the intersection with the plane of motion, these points form zero velocity curves (ZVCs). The zero velocity curves and surfaces separate regions of allowable and feasible motion, providing us insight into the possible itinerary for a spacecraft under natural motion within a multi-body dynamical system. Furthermore, such structures can provide insight into effective and appropriate use of a propulsion system. Although the CR3BP is autonomous, the resulting dynamical field is nonlinear and chaotic. Thus, trajectories within a Sun-Earth CR3BP may exhibit a large variety of geometries.

To effectively transition a trajectory from the CR3BP to a high-fidelity model, an ephemeris model that captures the point mass gravitational influence of the Sun, Earth and Moon and low-thrust acceleration, is useful. Each of these three bodies, with mass M_i, as well as the spacecraft, is located in an inertial frame, $\hat{X}\hat{Y}\hat{Z}$, with a fixed origin at point O. Then, we employ the same characteristic quantities used to nondimensionalize mass, time and length quantities in the Sun-Earth CR3BP. Each body P_j is located relative to another body P_i by the nondimensional inertial position vector $\bar{R}_{ij}$. Then, we can write the nondimensional equations of motion of the spacecraft relative to the Earth due to the gravity of the Sun, Earth and Moon, as well as a low-thrust acceleration, $\bar{a}_{LT}$, in the inertial frame as:

$$\ddot{\bar{R}}''_{E,sc} = \text{-}\frac{G(M_E+M_{SC})}{R^3_{E,sc}}\bar{R}_{E,sc} \quad (5)$$

$$+G\left[M_S\left(\frac{\bar{R}_{sc,S}}{R^3_{sc,S}}\text{-}\frac{\bar{R}_{E,S}}{R^3_{E,S}}\right) + M_M\left(\frac{\bar{R}_{sc,M}}{R^3_{sc,M}}\text{-}\frac{\bar{R}_{E,M}}{R^3_{E,M}}\right)\right] + \bar{a}_{LT}$$

where the subscript E identifies the Earth, sc corresponds to the spacecraft, M indicates the Moon and S corresponds to the Sun [18].

Simultaneously, the spacecraft mass must also be integrated via an additional differential equation corresponding to the mass flow rate. Prior to nondimensionalization, this mass flow rate is:

$$\dot{m} = \text{-}\frac{T_{lt}^2}{2P} \quad (6)$$

and

$$P = \frac{T_{lt} I_{sp} g_0}{2} \quad (7)$$

where P is the engine exhaust power, T_{lt} is the dimensional thrust, equal to 0.4 mN, I_{sp} is the specific impulse, equal to 1250s in this example, and g_0 is the gravitational acceleration measured on the surface of the Earth, 9.81 m/s. Then, the low-thrust acceleration term, $\bar{a}_{LT}$, is equal to the nondimensional thrust divided by the nondimensional spacecraft mass [18].

Dynamical Structures

Since the CR3BP is autonomous, trajectories in the rotating frame possess one of four forms: equilibrium points, periodic orbits, quasi-periodic orbits or chaos. Computation and characterization of the first three of these particular solutions via DST can offer us insight into the dynamics within the Sun-Earth system, which is valuable due to the absence of an analytical solution to the equations of motion.

Equilibrium points are constant solutions to the equations of motion that possess both a velocity and acceleration equal to zero. In the CR3BP, there are five well-known equilibrium points: three collinear points L_1, L_2 and L_3, and two triangular points L_4 and L_5. The Jacobi constant evaluated at each of these points is, respectively, in the Sun-Earth system: $C_J(L_1) \approx 3.000891$, $C_J(L_2) \approx 3.000887$, $C_J(L_3) \approx 3.000003$, $C_J(L_4) \approx C_J(L_5) = 2.999996$. The lower the Jacobi constant, the higher the energy corresponding to each equilibrium point. These locations, which exist only in the rotating frame, are theoretical locations in the CR3BP where a spacecraft could remain indefinitely. Of course, the CR3BP is only an approximation to the dynamics within the Sun-Earth system. Thus, while the equilibrium points themselves may not be used for trajectory design, solutions in their vicinity are valuable. For this mission example, we leverage motions in the vicinity of L_5 for a final science orbit. However, the collinear equilibrium points also provide us with useful information relevant to the trajectory design process. In fact, L_1 and L_2, which lie on the *x*-axis and on either side of the Earth in the Sun-Earth system, serve as "gateways" for motion to depart the Earth vicinity. Thus, we also make use of the characterization of the flow through these gateways as a necessary component of reaching L_5 from a deployment condition near the Earth during itinerary construction [21].

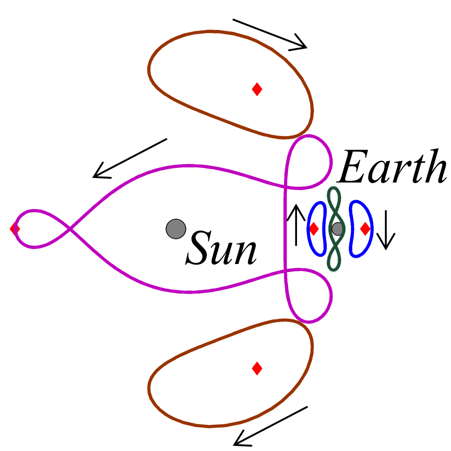

Figure 3. Sample periodic orbits in the SE CR3BP, with equilibrium points located via red diamonds.

In the autonomous CR3BP, an infinite variety of periodic orbits exist in families in various regions of the multi-body system [22]. These periodic orbits consist of motion that exactly repeats when viewed in a rotating frame, over a time labeled the orbit period, *T,* and can exist in various regions as depicted in Figure 3. We first compute a single periodic orbit numerically using correction algorithms such as multiple-shooting, collocation, or discrete variational mechanics. We then compute additional orbits along a family from a single solution via a numerical continuation method. While there are infinite families of periodic orbits, the orbits of interest for this investigation include simply-periodic orbits near SEL_2 and SEL_5.

Unstable periodic orbits admit manifold structures, corresponding to trajectories that naturally approach or depart the orbit. These manifolds can guide the behavior of trajectories within a multi-body system. For this mission design example, the manifolds associated with orbits near SEL_2, depicted in Figure 4 in a Sun-Earth rotating frame, are particularly useful in gaining a rapid and insightful understanding of motion that departs the Earth vicinity through the SEL_2 gateway and approaches the SEL_5 vicinity. Furthermore, we can straightforwardly compute, visualize, and characterize manifolds structures in the CR3BP. As a result, we can sample these manifolds to identify arcs at a desired energy level and with a desired geometry to construct an initial guess for a trajectory.

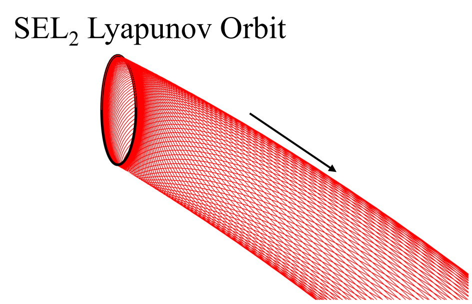

Figure 4. Unstable manifold associated with a Sun-Earth L_2 Lyapunov orbit in the CR3BP.

Corrections Procedure

To recover a continuous trajectory for the low-thrust-enabled CubeSat, a multiple-shooting method is employed for differential corrections [18]. This method begins by discretizing a trajectory into a sequence of nodes. Then, these nodes are simultaneously updated using an iterative numerical procedure to enforce continuity as well as any additional boundary conditions. This procedure is implemented in the low-thrust-enabled point mass ephemeris model of the Earth, Sun, and Moon. In this model, each node is described by the inertial state vector relative to the Earth, the time at each node, the integration time across the arc, the instantaneous spacecraft mass and, where applicable, the thrust direction unit vector. An additional constant vector defining whether the thrust is activated must also be stored. For this formulation, additional constraints are required. Over low-thrust-enabled arcs, the thrust vector variables must be constrained to be a unit vector, while the initial deployment state and epoch are fixed.

5. Results

Initial Guess Construction

To depart the Earth vicinity, and approach the desired mission orbit, we derive a general itinerary for trajectory construction from multi-body dynamical insight. In fact, trajectories that depart the Earth vicinity and reach SEL_5 must pass through either the SEL_1 or SEL_2 gateways. These gateways are depicted in Figure 5, in an Earth-centered rotating frame. The ZVCs are indicated with black lines, dividing regions of allowable (white) and forbidden (gray) motion, with Lagrange points located by green diamonds. The Earth is displayed in this figure, not to scale. To pass through these gateways in the SE CR3BP, the Jacobi constant along a trajectory must be, at least, below the Jacobi constant corresponding to either SEL_1 or SEL_2. If the value of the Jacobi constant is above that of L_1 or L_2, the spacecraft cannot depart the Earth vicinity through the associated gateway. Note that in a point mass ephemeris model, the Jacobi constant is not constant along a natural trajectory. However, it is still useful in gaining dynamical insight into the general geometry of a transfer trajectory.

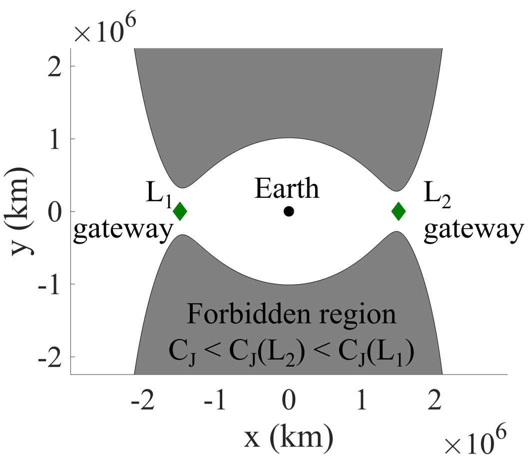

Figure 5. Definition of L_1 and L_2 gateways, visualized via the ZVCs indicating gray regions of forbidden motion.

The assumed deployment state, similar to a previous set of deployment conditions for the CubeSats riding onboard EM-1, corresponds to a high-energy trajectory that naturally departs the Earth vicinity through the SEL_2 gateway [17]. Immediately following deployment, the spacecraft performs a lunar flyby. Although the initial value of the Jacobi constant at deployment is equal to 3.0021, a lunar flyby dramatically reduces the Jacobi constant to 3.00036, well below the value of the Jacobi constant corresponding to SE L_2. To mitigate any unnecessary flight time and reduce the required maneuvering capability, we leverage the natural motion as much as possible. As a result, we design the low-thrust-enabled trajectory to ensure that it passes through the SEL_2 gateway with a Jacobi constant below that of L_2.

Activating the low-thrust engine in the velocity direction after deployment increases the energy of the spacecraft, but also reduces the flyby altitude. Aligning the thrust vector with the anti-velocity direction raises the flyby altitude – which is valuable for reducing the sensitivity of the trajectory to off-nominal conditions – such maneuvering also raises the Jacobi constant of the spacecraft evaluated in the SE CR3BP. Using these observations as a foundation, we apply four maneuvers in approximately the velocity direction, lasting two hours each and separated by approximately 10 hours, prior to the lunar flyby. Note that during corrections, the exact thrust direction along each arc can be slightly adjusted. We display the resulting trajectory in Figure 6 in a SE rotating frame with the coast arcs colored blue and the low-thrust-enabled arcs plotted in red, with arrows indicating direction of motion. These maneuvers are useful for on-orbit thruster validation while the spacecraft is still close to the Earth and are separated by ten hours, sufficient time for ground-based communication and operations. Furthermore, these planned maneuvers enable slight adjustments to the lunar flyby and, therefore, the post-flyby arc that naturally passes through the SEL_2 gateway.

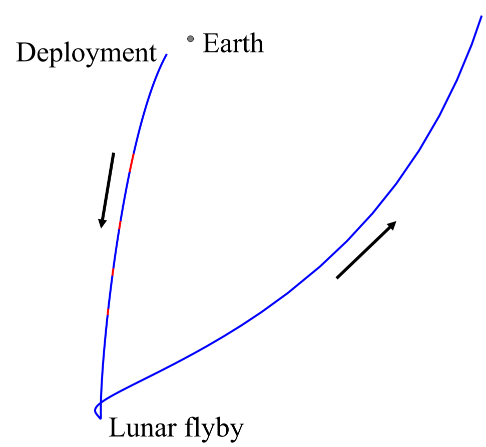

Figure 6. Following deployment and lunar flyby, the low-thrust enabled trajectory depicted in a SE rotating frame. This segment features four 2-hr low-thrust arcs where the thrust vector is directed along the velocity vector.

We must select a mission orbit near SEL_5. Since the post-flyby natural motion through the SEL_2 gateway possesses a relatively small component out of the ecliptic, selecting a planar mission orbit near SEL_5 offers a significant reduction in the solution space. Such motion includes short period and long period near SEL_5. However, to further reduce the size of the initial search space, we only consider the short period orbits in this investigation. We present some members of this family in Figure 7 in the Sun-Earth rotating frame. These short period orbits evolve away from SEL_5 and motion along each member of the family is clockwise around the equilibrium point. Members of this family exhibit sufficiently large revolutions around SEL_5, resembling the motion that naturally approaches the region from the Earth vicinity and, heuristically, guiding the search process towards a transfer that is feasible for a low-thrust-enabled mission. As members along the family evolve away from SEL_5, the Jacobi constant decreases from a limiting value of $C_J(L_5)$ = 2.999997 and the orbit period decreases from a limiting value equal to one period of the Earth in its orbit around the Sun, i.e., one year. Simultaneously, the distance of the spacecraft to the Sun decreases, increasing the radiation exposure.

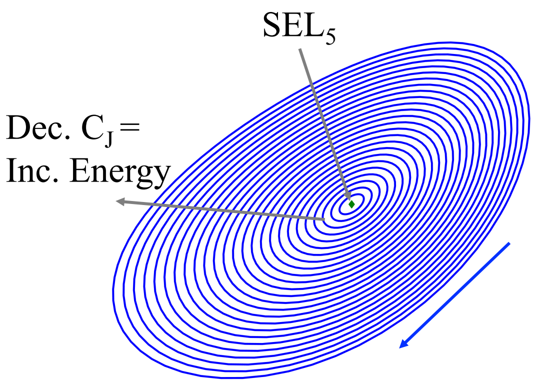

Figure 7. Sample members of the SEL5 short period family, emanating from the SEL5 equilibrium point. As the orbits evolve away from L5, the Jacobi constant decreases.

To reduce the required propellant mass and maneuver time to reach a SEL$_5$ periodic orbit from the post-flyby trajectory, which possesses a Jacobi constant between that of SEL$_2$ and SEL$_5$, it is valuable to maximize the Jacobi constant along the selected mission orbit. Achieving this goal corresponds to selecting a small SEL$_5$ short period orbit for use in constructing an initial guess for a trajectory that reaches the SEL$_5$ vicinity. Its orbit period is nearly equal to the period of the Sun and Earth in their assumed circular orbits. We can recover a trajectory that remains near SEL$_5$ for several years in a high-fidelity model by appending the existing initial guess with several revolutions of the selected short period orbit. Following application of a multiple shooting method, applied in the high-fidelity model, the exact short period motion may not necessarily be retained. However, bounded motion sufficiently close to the equilibrium point over a desired mission lifetime is still achieved.

Following the lunar flyby, the Jacobi constant is below that of SEL$_2$, but still above that of the SEL$_5$ short period family of orbits. Operationally, it is preferable to thrust close to the Earth, where possible, to support ground-based navigation tasks and early corrections to perturbed or off-nominal performance. Thus, to efficiently reduce the Jacobi constant to a value closer to that of the SEL$_5$ short period orbits, we activate the thruster in approximately the velocity direction prior to and during departure through the SEL$_2$ gateway. However, the reduction in Jacobi constant is at the expense of required propellant mass – we can achieve a balance between these two goals through the application of a multiple-shooting corrections scheme and, later, local optimization [18]. When the low-thrust engine is activated 29.4 days after deployment for a total of 87 days, the resulting trajectory is displayed in Figure 8 in the Sun-Earth rotating frame with coast (blue) and low-thrust (red) arcs. At the crossing of the L$_2$ gateway, the trajectory possesses a Jacobi constant equal to 3.00012 in the Sun-Earth CR3BP, between the Jacobi constants corresponding to L$_2$ and L$_5$. Including this low-thrust-enabled arc during trajectory construction also enables effective corrections to recover a continuous trajectory that is feasible within the limitations of the propulsive capability of a CubeSat.

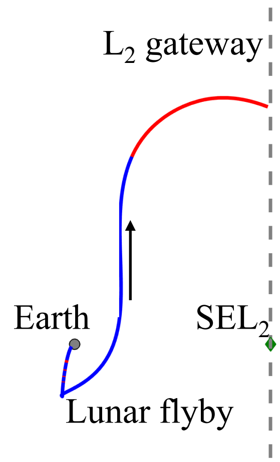

Figure 8. After the lunar flyby, the natural trajectory passes through the SEL$_2$ gateway, even with a low-thrust arc to lower the Jacobi constant.

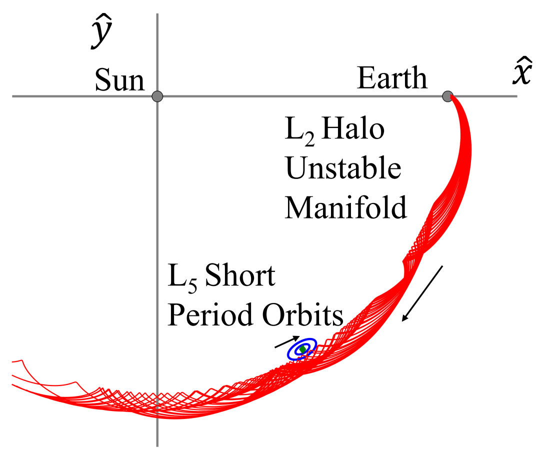

Figure 9. Unstable manifold structure associated with an SEL$_2$ halo orbit (red) with selected members of the SEL$_5$ short period family overlaid (blue), and plotted in the Sun-Earth rotating frame.

Finally, in the Sun-Earth CR3BP, natural motion through the SEL$_2$ gateway is guided by the manifolds of two-dimensional and three-dimensional orbits in the SEL$_2$ vicinity. Families with manifolds that influence motion through the gateway include the SEL$_2$ Lyapunov, halo, axial and vertical periodic and their associated quasi-periodic orbits. These manifolds are valuable in identifying arcs that connect the SEL$_2$ gateway to the SEL$_5$ vicinity. However, to reduce the computational complexity of capturing all motion through the gateway, some assumptions are useful. Following the lunar flyby, the spacecraft approaches the SEL$_2$ gateway with a small but nonzero and positive out-of-plane component. Thus, both the planar SEL_2 Lyapunov orbits and SEL_2 halo orbits with a small z-amplitude offer manifolds that may provide a suitable arc for initial guess construction, while also reducing the design space. Depicted in Figure 9 are a set of red trajectories that lie on the unstable manifold associated with a SEL_2 halo orbit, and displayed in the SE rotating frame. Overlaid on this plot are members of the SEL_5 short period family (blue), indicating the value of leveraging unstable manifold structures to identify arcs useful in initial guess construction.

While the trajectories along the unstable manifold travel through the same regions of the Sun-Earth system, they possess different geometries. In fact, as viewed in a Sun-Earth rotating frame, the trajectories exhibit oscillations in the distance from the Sun, with local minima corresponding to locations where the velocity magnitude approaches or is equal to a value of zero in the SE rotating frame. Near these regions, the spacecraft travels slowly and the time of flight is significantly increased. Although each arc in Figure 9 possesses the same Jacobi constant, trajectories with a larger number of oscillations in the distance to the Sun take a significantly longer time to approach the SEL_5 vicinity than a trajectory with one or two oscillations. Such dynamical insight can guide an exploration of the trajectory design space. For a CubeSat-enabled science mission, it may be preferable to reduce the time of flight. Thus, during initial guess construction, a manifold arc with fewer oscillations in the rotating frame may support rapid recovery of an end-to-end trajectory with a lower flight time.

Leveraging these insights from DST, we can construct a discontinuous initial guess from the individual, predominantly natural arcs within each of the described phases: 1) deployment through lunar flyby until reaching the SEL_2 gateway, recovered in a low-thrust-enabled point mass ephemeris model; 2) a natural trajectory along the unstable manifold of a SEL_2 halo orbit identified in the CR3BP; and 3) short period motion near SEL_5.

We reduce the discontinuities between neighboring arcs during multiple shooting through the introduction of low-thrust segments at the beginning and end of each natural arc. To connect the post-flyby arc with the manifold trajectory, we employ an 87-day low-thrust arc with the thruster direction aligned with the velocity vector in the initial guess. In addition, to connect the unstable manifold arc with the SEL_5 short period motion, we introduce a two-year thrust arc. Along this connection arc, the thruster direction is defined by the unit vector $\hat{u} = -0.9\hat{V} - 0.436\hat{N}$ where $\hat{V}$ indicates a unit vector in the velocity direction relative to the Earth and $\hat{N}$ corresponds to the orbit normal. We select this initial guess for the thruster direction to both reduce the speed of the spacecraft on approach to the SEL_5 region, and to reduce the out-of-plane component of the arc associated with the three-dimensional SEL_2 halo unstable manifold. This reduction in the z-component along the trajectory reduces the amplitude of the natural out-of-plane oscillations along the transfer to match those of the natural motion around SEL_5 in a point mass ephemeris model.

Prior to corrections, the constructed initial guess must be discretized. Each segment is discretized into arcs using nodes that are evenly spaced in time and sufficiently enable the corrections algorithm to update the solution during each iteration. Since the corrections algorithm leverages a Newton's method, as well as a state transition matrix that reflects the sensitivity of each arc to updates to the node at the beginning of the corresponding arc, too few nodes creates challenges in effective recovery of a continuous solution. Too fine a discretization, however, results in an increased computational load. Thus, the discretization of each segment is an iterative and interactive process. Furthermore, low-thrust-enabled segments along the initial guess are divided into a sequence of arcs over which the thruster direction is held constant in a velocity-normal-conormal frame, using the Earth as the origin. The number of arcs along each low-thrust-enabled segment can be increased to provide greater flexibility in recovering a continuous solution between deployment and the SEL_5 region. However, the number of arcs along each low-thrust segment, and the time between each node, must support operational feasibility of changing the thruster direction or frequency of sending thrust commands to the spacecraft. The resulting discontinuous initial guess is displayed in Figure 10 in the Sun-Earth rotating frame. Blue arcs indicate natural motion, while red arcs correspond to the low-thrust-enabled motion.

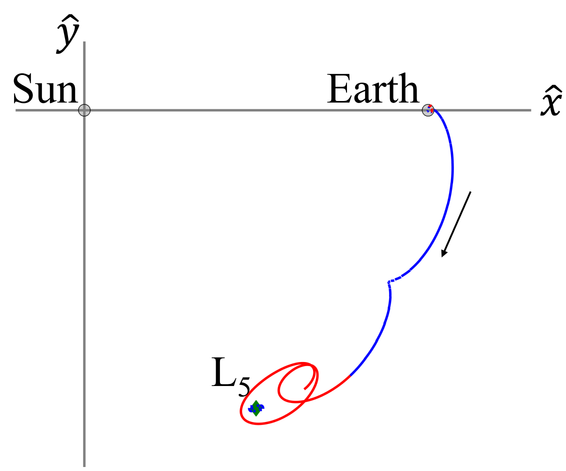

Figure 10. Discontinuous initial guess for a trajectory constructed for a 14kg CubeSat with a 0.4 mN low-thrust engine from a previous set of EM-1 deployment conditions to SEL_5.

Recovering an End-to-End Trajectory

We input the constructed initial guess into a corrections algorithm, enforcing continuity in a point mass ephemeris model of the gravitational influence of the Sun, Earth and Moon, while also capturing the additional acceleration of the low-thrust propulsion system. Furthermore, the deployment state and epoch are fixed. Following corrections, we recover a continuous end-to-end trajectory, as displayed in Figure 11 in the Sun-Earth rotating frame with blue arcs indicating natural motion and red arcs depicted low-thrust-enabled arcs. A zoomed-in view near the Earth appears in Figure 12. For the trajectory constructed in this example, the lunar flyby altitude is approximately 1135 km. The constructed solution also possesses long low-thrust arcs that may create operational challenges. In fact, the power capability of CubeSats limits the onboard operations: since significant power is needed to activate the low-thrust engine, other operations such as navigation or science may not occur simultaneously. Rather, subsequent analyses should incorporate shorter thrusting arcs separated by brief coasting segments. Such solutions likely exist close to the constructed trajectory and still retain the desired geometry.

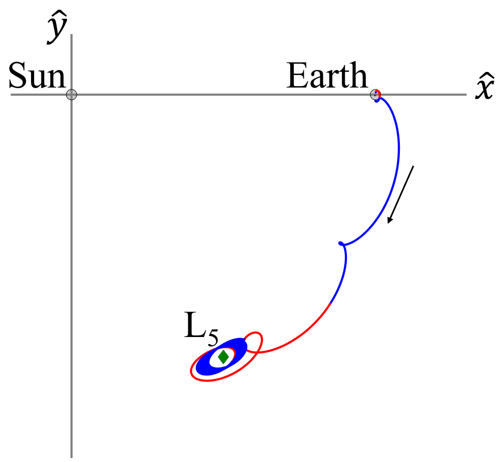

Figure 11. Continuous sample trajectory constructed for a 14kg CubeSat with a 0.4 mN low-thrust engine from a previous set of EM-1 deployment conditions to SEL$_5$.

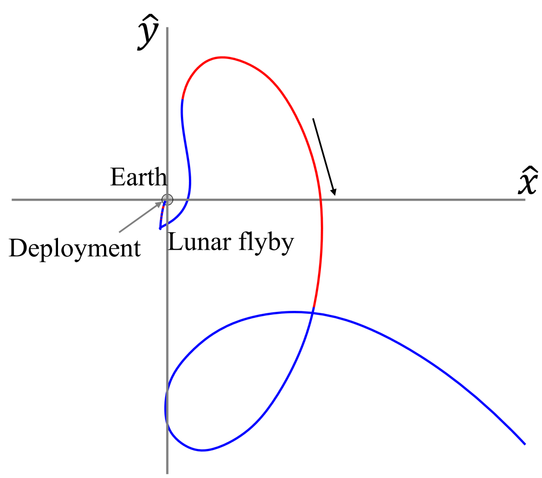

Figure 12. Zoomed-in-view of the post-deployment and lunar flyby segment of the trajectory.

The recovered trajectory delivers the 14 kg CubeSat from a high-energy deployment state to the SEL$_5$ region, via application of the 0.4mN low-thrust engine and the use of natural multi-body dynamical structures. This transfer requires a time of flight of 4.2 years to reach the SEL$_5$ region from a fixed EM-1 deployment condition, and a propellant mass of 2.35 kg, thus meeting the constraints we imposed on this design problem. This time of flight is a direct result of the assumed deployment conditions and limited propulsive capability, as well as the geometry of the constructed initial guess. Once in the SEL$_5$ vicinity, the spacecraft motion is bounded and encircles the equilibrium point eight times, corresponding to approximately eight years in the desired science orbit. Additional revolutions of a short period orbit may be appended to the initial guess to recover bounded motion near SE L_5 over a longer time interval. Furthermore, as explained in the science motivation section, since the spacecraft would be trailing the Earth throughout the majority of this cruise time, it could still achieve all its science goals while on its outbound trajectory. Of course, an expansive search of the design space, via dynamical systems theory, may reveal trajectories with shorter flight times and/or a lower propellant mass usage. Such a search is warranted in future investigation, along with expansion to explore the design space associated with trajectories for the "Upper End" spacecraft option, corresponding to a SmallSat. In addition, the impact of alternative deployment conditions on the propellant usage and flight time are also valuable. Nevertheless, this sample trajectory demonstrates the value of a dynamical systems approach to identifying feasible transfers for a low-thrust-enabled CubeSat mission.

6. SUMMARY

In this paper, we presented the science motivation behind a potential SmallSat or CubeSat mission to the SEL$_5$ region. Today, the main constraint in enabling small missions to reach these distant points is the amount of propulsive capability required. Therefore, we then investigated the state-of-the-art in SmallSat propulsion and power technology to offer constraints on the trajectory design out to these points. We then described an informed approach to trajectory design, using DST, to investigate previously undiscovered low-thrust trajectories destined for SEL$_5$. Finally, we presented an initial trajectory to this Lagrange point that could be achieved with a 14kg CubeSat with < 4kg of propellant. This sample trajectory demonstrates the value of this method, and future work will further explore the trajectory design space.

ACKNOWLEDGEMENTS

Part of this research was carried out at the Jet Propulsion Laboratory, California Institute of Technology, under a contract with the National Aeronautics and Space Administration and funded through the Internal Strategic University Research Partnerships (SURP) program. Part of this research was also performed at the University of Colorado Boulder.

REFERENCES

[1] Space Studies Board. Solar and Space Physics: A Science for a Technological Society. National Academies Press, 2013.

[2] Kaiser, Michael L., et al. "The STEREO mission: An introduction." Space Science Reviews 136.1-4 (2008): 5-16.

[3] Webb, D. F., Howard, T. A.: 2012, Coronal Mass Ejections: Observations, Living Rev. Sol. Phys., 9, 3

[4] F. Alibay, J.C. Kasper, T.J.W. Lazio, and T. Neilsen, Sun Radio Interferometer Space Experiment (SunRISE): Tracking Particle Acceleration and Transport in the Inner Heliosphere, 2017 IEEE Aerospace Conference Proceedings, Big Sky, MT, 2017.

[5] Vourlidas, A. (2015), Mission to the Sun-Earth L5 Lagrangian Point: An Optimal Platform for Space Weather Research, Space Weather, 13, 197–201, doi:10.1002/2015SW001173.

[6] Gopalswamy N., et al.: 2011b, Earth-Affecting Solar Causes Observatory (EASCO): A potential International Living with a Star Mission from Sun–Earth L5, J. Atmos. Sol.-Terr. Phys., 73, 658- 663.

[7] Schmidt, W. K. H., Bothmer, V.: 1996, Stereoscopic viewing of solar coronal and interplanetary activity, Adv. Space Res., 17, 4/5, 369-376.

[8] Akioka, M., Nagatsuma, T., Miyake, W., Ohtaka, K., Marubashi, K.: 2005, The L5 mission for space weather forecasting, Adv. Space Res., 35, 65–69.

[9] Lavraud, B. et al.: 2016, A small mission concept to the Sun-Earth Lagrangian L5 point for innovative solar, heliophysics, and space weather science, Journal of Atmospheric and Solar-Terrestrial Physics 146, 171-185.

[10] Accion Systems, TILE – Tiled Ionic Liquid Electrospray, http://www.accion-systems.com/tile, retrieved October 9th 2017.

[11] Busek, BHT-200 Busek Hall Effect Thruster, http://www.busek.com/index_htm_files/70000700%20BHT-200%20Data%20Sheet%20Rev-.pdf, retrieved October 9th 2017.

[12] Aerojet, Electric Propulsion Data Sheets, https://www.rocket.com/files/aerojet/documents/Capabilities/PDFs/Electric%20Propulsion%20Data%20Sheets.pdf, retrieved October 9th 2017.

[13] Mueller, J. et al., A survey of micro-thrust propulsion options for microspacecraft and formation flying missions." 5th Annual CubeSat Developers Workshop San Luis Obispo, CA. 2008.

[14] MMA Design LLC, http://mmadesignllc.com/, retrieved October 9th 2017.

[15] Orbital ATK, Ultraflex Solar Array Systems, https://www.orbitalatk.com/space-systems/space-components/solar-arrays/docs/UltraFlex_Factsheet.pdf , retrieved October 9th 2017.

[16] Kamhawi, H., et al, Overview of Iodine Propellant Hall Thruster Development Activities at NASA Glenn Research Center, 52nd AIAA JPC AIAA- 2016-4729.

[17] Bosanac, N., Cox, A., Howell, K.C., Folta, D.C., Trajectory Design for a Cislunar CubeSat Leveraging Dynamical Systems Techniques: The Lunar IceCube Mission, In press, Acta Astronautica.

[18] Bosanac, N, Leveraging Natural Dynamical Structures to Explore Multi-Body Systems, Ph.D. Dissertation, Purdue University, August 2016.

[19] Bosanac, N., Webster, C.M., Howell, K.C., Folta, D.C., Trajectory Design and Station-Keeping Analysis for the Wide Field Infrared Survey Telescope Mission, AAS/AIAA Astrodynamics Specialist Conference, Stevenson, WA, Aug 21 - 24, 2017.

[20] V. Szebehely, Theory of Orbits: The Restricted Problem of Three Bodies. London, UK: Academic Press, 1967.

[21] Folta, D., Bosanac, N., Cox, A., and Howell, K.C., The Lunar IceCube Mission Challenge: Attaining Science Orbit Parameters from a Constrained Approach Trajectory, 27th AAS/AIAA Space Flight Mechanics Meeting, San Antonio, Texas, February 5-9, 2017.

[22] Guzzetti, D., Bosanac, N., Haapala, A., Howell, K., and Folta, D., "Rapid Trajectory Design in the Earth-Moon Ephemeris System via an Interactive Catalog of Periodic and Quasi-Periodic Orbits," IAF 66th International Astronautical Congress, Jerusalem, Israel, October 12-16, 2015.

BIOGRAPHY

Farah Alibay *received her Bachelor's and Master's degrees from the University of Cambridge in 2010, both in Aerospace and Aerothermal Engineering. She received her PhD in Space Systems Engineering from the Massachusetts Institute of Technology in 2014. Her primary research focused on spatially and temporally distributed multi-vehicle architectures for planetary exploration. She is now a Systems Engineer at the Jet Propulsion Laboratory where she is current a Payload Systems Engineer on the InSight Mars Lander.*

Natasha Bosanac *received her Bachelor's degree from the Massachusetts Institute of Technology in 2010. She then received her Master's degree and Ph.D. in Aerospace Engineering in 2012 and 2016 from Purdue University, with a specialization in Astrodynamics. Her research focus is leveraging multi-body dynamics to enable space exploration for large spacecraft and SmallSats, both individual and in formations. She is currently an Assistant Professor in the Colorado Center for Astrodynamics Research and Smead Department of Aerospace Engineering Sciences at the University of Colorado Boulder.*

Jeffrey Stuart *received his B.S., M.S., and Ph.D. in Aeronautics & Astronautics from Purdue University in 2008, 2011, and 2014, respectively. He is currently research staff in Mission Design & Navigation at the Jet Propulsion Laboratory, California Institute of Technology. His interests include automated trajectory design, advanced navigation techniques, combinatorial optimization, and visual analytic methods.*